Modeling, Simulation, and Experimental Study of a Simulated Moving Bed Reactor for the Synthesis of Methyl Acetate Ester

Weifang Yu, K. Hidajat, and Ajay K. Ray*

Department of Chemical and Environmental Engineering, National University of Singapore, 10 Kent Ridge Crescent, Singapore 119260

In this work, the performance of a simulated moving bed reactor (SMBR) for the synthesis of methyl acetate catalyzed by Amberlyst 15 ion-exchange resin was evaluated numerically and experimentally. A rigorous mathematical model was developed to describe the dynamic behavior of SMBR and validated experimentally at different operating conditions. It was found that the model could predict the experimental results quite well. A high yield and purity of methyl acetate and nearly complete conversion of the limiting reactant, acetic acid, could be achieved in the SMBR by selecting proper operating conditions. The effects of various process parameters such as switching time, feed, eluent flow rate, etc., on the behavior of the SMBR was also investigated systematically.

Introduction

The simulated moving bed reactor (SMBR), in which chemical reaction and separation take place concurrently, has been gaining significant attention in recent years. The coupling of two unit operations in an SMBR not only improves the process economics by reducing capital and operating cost but also allows for higher conversions for equilibrium-limited reactions through the in-situ separation of the products, resulting in better yields and selectivities compared to those obtained with conventional processes. Studies have been carried out to evaluate the applicability of SMBRs to several classes of reactions, such as esterification,[1−5] etherification,[6] hydrogenation,[7−10] and isomerization,[11,12] as well as reactions involving sugar.[13,14] These works show that substantial improvements in process performance can be achieved in SMBRs compared to fixed-bed operation and that the application of SMBRs to the production of some fine chemicals and pharmaceuticals is promising. However, because of the complexity of SMBR processes, there are very few applications of SMBRs in the chemical industry. A more detailed understanding and criteria for the operation of SMBRs is needed before successful applications can be achieved. In this work, the synthesis of methyl acetate (MeOAc) ester catalyzed by Amberlyst 15 is considered to investigate the performance of SMBRs and obtain deeper insight into the behavior of the processes occurring therein. A mathematical model is developed and then solved using experimentally determined kinetic and adsorption parameters. The SMBR model-predicted results are verified experimentally, and finally, sensitivity studies are performed to investigate the effects of various parameters on the performance of the integrated reactor−separator.

Direct Synthesis of Methyl Acetate in an SMBR

The overall esterification reaction of interest can be described by the equation

$$CH_3COOH + CH_3OH \rightleftharpoons CH_3COOCH_3 + H_2O \quad (1)$$

In the reactor, methanol is used as the carrier solvent and is present in excess. The methanol concentration varies very little during the entire reaction process and, therefore, can be regarded as constant. The breakthrough curves of the reactants and products from a single packed column were experimentally measured at different temperatures, feed concentrations, and flow rates. The experimental results showed that H_2O travels more slowly than MeOAc (less strongly adsorbed); the reaction rate increases with increasing reaction temperature; and the conversion of the limiting reactant, acetic acid (HOAc), is favored at high temperature and at low flow rate. The adsorption equilibrium constants and reaction kinetic parameters, together with their dependence on temperature, were determined experimentally and reported elsewhere.[15]

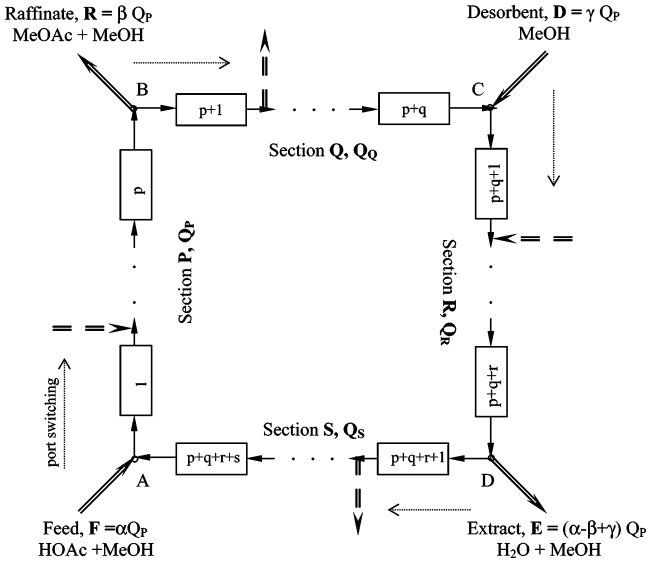

Figure 1. Schematic diagram of a SMBR system. The inlets and outlets divide the entire system into four sections: P, Q, R, and S with *p*, *q*, *r*, and *s* columns, respectively. The flow rates in the various sections are given by $Q_Q = (1 - \beta)Q_P$, $Q_R = (1 - \beta + \gamma)Q_P$, and $Q_S = (1 - \alpha)Q_P$, where α, β, $\alpha\nu\delta$ γ are given by F/Q_P, R/Q_P, and D/Q_P, respectively.

Figure 1 shows a four-section SMBR system in which all input/output ports shift by one column in unison in the direction of fluid flow after a fixed interval (switch-

* To whom correspondence should be addressed. Tel.: . +65 6874 8049. Fax: +65 6779 1936. E-mail: cheakr@nus.edu.sg.

10.1021/ie0302241 CCC: $25.00
Published on Web 11/13/2003

ing time, t_s). To achieve a good separation, each section should fulfill its own role, which is determined by the length (L_{col}) and number (N_{col}) of columns, the fluid flow rate (Q) in each section, and the switching time (t_s). Section R has the highest flow rate, Q_R, to desorb the strongly adsorbed component (water) so that at least the first column of this section is clean before the next port switching is done. The difficulties in this task include insufficient fluid flow rates Q_R, short switching intervals, and long columns, as well as axial dispersion and tailing of the desorbing concentration front. The column flow rate in section S, Q_S, is lower than Q_R after water has been withdrawn as (extract) product at the rate of $Q_R - Q_S$. However, Q_S should be large enough to desorb ester from section S to be mixed with feed as the recycle to section P. At the same time, water should be retained in section S. The difficulties in the task of this section are similar to those for section R, but the influence of axial dispersion is more significant because of the concentration shock caused by the introduction of feed at the end of section S. The main task of section P is to retain the strongly adsorbed component (i.e., H_2O), so that this component does not break through at the raffinate port where ester is collected as the product. The possible difficulties in this section result from the high column fluid flow rate (Q_P), small section length (pL_{col}), long switching time, and axial dispersion. Part of the ester flows into section Q, where the column flow rate, Q_Q, should be low enough to prevent ester from breaking through into section R. The primary roles of section Q are, therefore, retention of ester and desorption of methanol to be mixed with the desorbent stream and recycled to section R.

Sections S and P should be long enough to prevent water from breaking through into section P and at the raffinate port, respectively, as the primary objective for methyl acetate synthesis is to maximize the purity and yield of the ester. The roles of sections Q and R are to retain ester and desorb water, respectively. However, given that the primary objective in methyl acetate synthesis is not necessarily to achieve a high purity of H_2O at the extract port, the columns in these two sections could be short, and one column might be sufficient for each of these two sections. In general, because all columns are of identical length (as required in the design of an SMBR), it would be advantageous if the columns were shorter in length but larger in numbers, so that they could be distributed in each section optimally to achieve the desired objectives.

The effects of reaction and separation in an SMBR are interrelated. On-site separation of the two products, ester and water, promotes the conversion of the limiting reactant, acetic acid, and near-complete reaction (high conversion) favors a high purity of the ester at the raffinate port. If the conversion of acid is low, unconverted acid is more likely to pollute the ester at the raffinate port. The conversion of acetic acid is enhanced in SMBRs through in situ product separation, as well as through an increase in the residence time of the acid because the esterification reaction is kinetically controlled.

Mathematical Model

A comprehensive analysis of the performance of SMBRs will be difficult through only experimental study because of the complexity of the process. Particularly, the length and number of columns in each section, flow rates of different streams in various sections, and switching time are impossible to determine in advance without a detailed mathematical or optimization study. Consequently, a dynamic mathematical model was developed not only to acquire a deeper understanding of the behavior of the reactor, but also to enable the design of an experimental setup and the efficient completion of experiments.

The concentration of methanol remains essentially unchanged in the course of reaction, as methanol acts as both a reactant and a carrier solvent and is present in large excess. The reaction rate equation is described by a quasihomogeneous kinetic model[15−17] and is written as

$$R = k_f\left(q_{HOAc} - \frac{q_{MeOAc}q_{H_2O}}{K_e}\right) \tag{2}$$

where R denotes the reaction rate, q_i is the concentration of component i (MeOAc, H_2O, or HOAc) in the solid phase, k_f is the forward reaction rate constant, and K_e represents the reaction equilibrium constant. The concentration of adsorbed species i in the solid phase is computed by assuming that the local liquid and solid phases are in equilibrium and a linear adsorption isotherm is applicable. Therefore, it is expressed as

$$q_i = K_i C_i \tag{3}$$

where K_i and C_i are the adsorption equilibrium constant and liquid-phase concentration of component i, respectively. It should be noted that the linear isotherm is valid only when the concentrations of the adsorbed components are low in the bulk liquid phase, as is the case in this study. When the concentrations of the reactants and products are not sufficiently low, nonlinear adsorption models, such as the Langmuir model, should be considered to describe adsorption process accurately.

On the basis of the proposed reaction kinetics and adsorption isotherms, the dynamic model for a fixed-bed chromatographic reactor corresponding to each single column in the SMBR unit was developed by adopting an equilibrium-dispersive model. The mass balance equation for each component i is written as follows

$$\frac{\partial C_i}{\partial t} + \left(\frac{1-\epsilon}{\epsilon}\right)\frac{\partial q_i}{\partial t} + \frac{u}{\epsilon}\frac{\partial C_i}{\partial z} - \left(\frac{1-\epsilon}{\epsilon}\right)v_i R = D_{iM}\frac{\partial^2 C_i}{\partial z^2} \tag{4}$$

The initial and boundary conditions are

$$C_i(t=0) = C_i^0 \tag{5a}$$

$$C_i(0<t<t_p)_{z=0} = C_{f,i} \tag{5b}$$

$$C_i(t>t_p)_{z=0} = 0 \tag{5c}$$

$$\left(\frac{\partial C_i(t)}{\partial z}\right)_{z=0} = 0 \tag{5d}$$

The kinetic and adsorption constants and diffusion coefficients of each component involved in the process are listed in Table 1. They were determined semiempirically by fitting the experimentally measured breakthrough curves with model predictions obtained

by solving the above mass balance equations. The detailed procedure is described elsewhere.[15]

An SMBR unit resembles a fixed-bed chromatographic reactor except at the instant of column rotation. Therefore, the dynamic behavior of the SMBR unit can be described by the mathematical model of a single reactive chromatographic column that also incorporates cyclic port switching. The modified mass equations are given by

$$\frac{\partial C_{ij}^{(N)}}{\partial t} + \left(\frac{1-\epsilon}{\epsilon}\right)\frac{\partial q_{ij}^{(N)}}{\partial t} + \frac{u_\phi}{\epsilon}\frac{\partial C_{ij}^{(N)}}{\partial z} - \left(\frac{1-\epsilon}{\epsilon}\right)\nu_i R_j^{(N)} = D_i \frac{\partial^2 C_{ij}^{(N)}}{\partial z^2} \quad (6)$$

for component i in the jth column during the Nth switching period, where u_ϕ denotes the superficial flow rate in section ϕ (with ϕ = P, Q, R, S) and the reaction rate expression and adsorption isotherms are given by

$$R_j^{(N)} = k_f\left(q_{\mathrm{HOAc},j}^{(N)} - \frac{q_{\mathrm{MeOAc},j}^{(N)}\, q_{\mathrm{H_2O},j}^{(N)}}{K_e}\right) \quad (7)$$

$$q_{ij}^{(N)} = K_i C_{ij}^{(N)} \quad (8)$$

The initial and boundary conditions are

Initial conditions

$$\text{When } N = 0, \quad C_{ij}^{(0)} = C_{ij}^{\text{initial}} = 0 \quad (9a)$$

$$\text{When } N \geq 1, \quad C_{ij}^{(N)} = C_{i,j+1}^{(N-1)} \quad \text{for} \quad j = 1, \ldots, (N_{col} - 1) \quad (9b)$$

$$C_{ij}^{(N)} = C_{i1}^{(N-1)} \quad \text{for} \quad j = N_{col} \quad (9c)$$

Boundary conditions

Feed entry point (point A in Figure 1)

$$C_{i1}^{(N)}|_{z=0} = (1-\alpha)C_{i,N_{col}}^{(N)}|_{z=L} + \alpha C_{i,f} \quad (10a)$$

Raffinate takeoff point (point B in Figure 1)

$$C_{i,p+1}^{(N)}|_{z=0} = C_{i,p}^{(N)}|_{z=L} \quad (10b)$$

Eluent inlet point (point C in Figure 1)

$$C_{i,p+q+1}^{(N)}|_{z=0} = \left(\frac{1-\beta}{1-\beta+\gamma}\right)C_{i,p+q}^{(N)}|_{z=L} \quad (10c)$$

Extract takeoff point (point D in Figure 1)

$$C_{i,p+q+r+1}^{(N)}|_{z=0} = C_{i,p+q+r}^{(N)}|_{z=L} \quad (10d)$$

The mass balance (eq 6), initial (eq 9) and boundary (eq 10) conditions, kinetic equation (eq 7), and adsorption isotherm (eq 8) completely define the SMBR system. The PDEs were solved using method of lines. The PDEs were first discretized in space using the finite difference method (FDM) to convert them into a set of several coupled ODE-IVPs, and the resultant stiff ODEs of the initial value kind were solved using the subroutine DIVPAG in the IMSL library. Because periodic switching is imposed on the system, the reactor works under transient conditions. Whenever switching is performed, a new initial value problem must be solved. However, a cyclic (periodic) steady state with a period equal to the switching time is eventually attained. After each switching, column numbering was redefined according to eq 11, so that feed is always introduced into the first column.

before switching	after switching
column 1	column N_{col}
column j	column $j-1$

$$j = 2, 3, \ldots, N_{col} \quad (11)$$

The concentration profiles were obtained from the solution of the above equations (eqs 6−11). The objectives of this work are to determine whether we can achieve a higher conversion and improve product purity for MeOAc synthesis in an SMBR. Therefore, the design of the SMBR configuration and operating conditions to be used therein must be set such that conversion of the limiting reactant HOAc (X_{HOAc}) and the yield (Y_{MeOAc}), purity (P_{MeOAc}), and selectivity (S_{MeOAc}) of the desired product (MeOAc) are maximized at the raffinate port. The four quantities are defined as follows

$$X_{HOAc} = [(\text{HOAc fed} - \text{HOAc collected at raffinate and extract})]/[\text{HOAc fed}]$$
$$= \{\alpha C_{HOAc,f}\, t_s - [\beta \int_0^{t_s} C_{HOAc,p}^{(N)}|_{z=L_{col}}\, dt + (\alpha+\gamma-\beta)\int_0^{t_s} C_{HOAc,p+q+r}^{(N)}|_{z=L_{col}}\, dt]\}/\alpha C_{HOAc,f} t_s \quad (12)$$

$$Y_{MeOAc} = \frac{\text{MeOAc collected in raffinate}}{\text{HOAc fed}} = \frac{\beta(\int_0^{t_s} C_{MeOAc,p}^{(N)}|_{z=L_{col}}\, dt]}{\alpha C_{HOAc,f} t_s} \quad (13)$$

$$P_{MeOAc} = \frac{\text{MeOAc collected in the raffinate}}{(\text{MeOAc} + H_2O + \text{HOAc}) \text{ collected in the raffinate}} = \frac{\int_0^{t_s} C_{MeOAc,,p}^{(N)}|_{z=L_{col}}\, dt}{\int_0^{t_s} (C_{MeOAc,p}^{(N)} + C_{H_2O,p}^{(N)} + C_{HOAc,p}^{(N)})|_{z=L_{col}}\, dt} \quad (14)$$

$$S_{MeOAc} = \frac{\text{MeOAc collected in the raffinate}}{(\text{MeOAc} + H_2O) \text{ collected in the raffinate}} = \frac{\int_0^{t_s} C_{MeOAc,p}^{(N)}|_{z=L_{col}}\, dt}{\int_0^{t_s} (C_{MeOAc,p}^{(N)} + C_{H_2O,p}^{(N)})|_{z=L_{col}}\, dt} \quad (15)$$

To achieve separation between the components, the internal flow rates of the fluid phases within the four sections and the switching time (which defines the hypothetical solid-phase velocity) have to be specified appropriately. For a true countercurrent moving bed chromatographic reactor (CMCR), Petroulas et al.[18] defined a parameter σ_i, called the relative carrying

Table 1. Adsorption Constant K_i, Kinetic Parameters k_f and K, and Dispersion Coefficients D_i[a]

T (K)	K_{MeOAc}	K_{H_2O}	K_{HOAc}	$10^6 D_{MeOAc}$ (m^2/s)	$10^6 D_{MeOH}$ (m^2/s)	$10^2 k_f$ (s^{-1})	K_e (mol/L)	X_e (%)	Y_e (%)	P_e (%)
313	0.40	3.08	0.48	5.01	14.58	1.42	349	98.57	98.57	49.64
318	0.38	2.94	0.43	3.88	11.17	1.77	334	98.49	98.49	49.62
323	0.36	2.78	0.38	3.46	11.03	2.40	325	98.43	98.43	49.60

[a] Calculations based on $[HOAc]_o = 2.0$ mol/L. $X_A = 1 - [HOAc]_{out}/[HOAc]_o$, $Y_E = [MeOAc]_{out}/[HOAc]_o$, $P_E = [MeOAc]_{out}/([MeOAc]_{out} + [HOAc]_{out} + [H_2O]_{out})$.

capacity of the solid relative to the fluid stream for any component i, as

$$\sigma_i = \frac{1-\epsilon}{\epsilon} NK_i \frac{u_s}{u_g} = \delta_i \frac{u_s}{u_g} \tag{16}$$

They showed that, to achieve countercurrent separation between two components, one must set σ greater than 1 for one component and less than 1 for the other. Later, Fish et al.[19] verified the above fact experimentally. Fish et al.[19] also defined V_i, the net velocity at which component i travels (or the concentration front moves) within the column, which, for a linear isotherm, is given by

$$V_i = \frac{u_g(1-\sigma_i)}{(1+\delta_i)} \tag{17}$$

Therefore, when $\sigma_i < 1$, $V_i > 0$ (species move with the fluid phase), and when $\sigma_i > 1$, $V_i < 0$ (species move with the solid phase). $\sigma = 0$ represents a fixed bed. Ray et al.[7,8] redefined the above parameter, σ, for an SCMCR by replacing the solid-phase velocity, u_s, in the CMCR by a hypothetical solid-phase velocity, ζ, defined as $\zeta = L/t_s$ for the SCMCR. They found, both theoretically[10] and experimentally,[9] that simulation of the countercurrent movement between two components can be achieved when the redefined σ's are set such that the value is greater than 1 for one component and less than 1 for the other component. Hence, in the present study, if we set σ properly, the more strongly adsorbed component (H_2O) will move with the imaginary solid (resin) stream and can be collected at the extract port (point D in Figure 1), while at the same time, the less strongly adsorbed component (MeOAc) will travel with the fluid stream and can be collected at the raffinate port (point B in Figure 1). It should also be noted that the parameter σ defined by the research group of Carr and Aris[18] is equivalent to β defined by the research group of Hashimoto,[2] γ defined by the research group of Ruthven,[20] and m defined by the research group of Morbidelli.[1]

Experimental Details

An experimental investigation of the SMBR would prove valuable for testing the model predictions. Theoretical analysis of the model of the SMBR has shown that, if an equilibrium-limited reaction occurs on the solid surface, then, under certain operating conditions, the chemical reaction process and the adsorption process interact to break the local thermodynamic equilibrium limitation, and it is possible to obtain improved conversions and product purity than would be obtained in a traditional fixed-bed reactor.[8] The aim of this experimental investigation is to achieve four objectives. The first is to determine whether the SMBR can produce pure product at a higher conversion than the fixed-bed reactor for a given reactor length, switching time, and eluent flow rates, as predicted by the model. The second is to compare the experimental results with the model predictions and determine how good is the model. The third is to characterize the effect of changing variables on the overall performance of the SMBR and to ascertain the robustness of the model. This would also verify whether the adsorption and kinetic parameters previously obtained experimentally[15] were correct. Finally, the fourth is to perform experiments at optimal operating conditions to determine whether the optimization results[21] are meaningful and attainable experimentally.

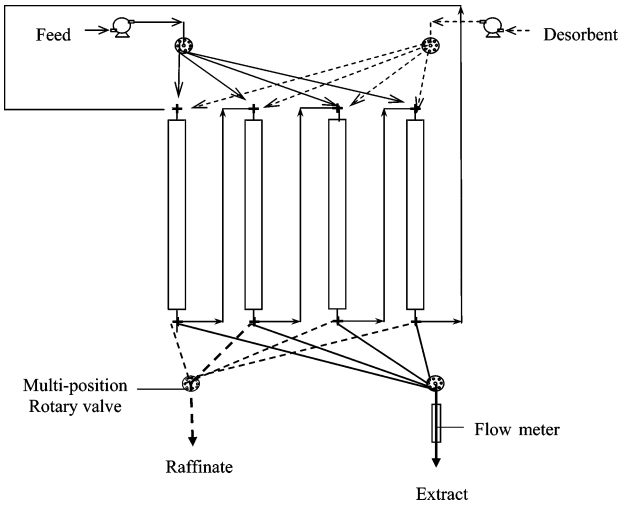

Figure 2. Schematic diagram of a four-column experimental apparatus.

For laboratory-scale experimental studies, the most convenient way to configure an SMBR is to design a reactor configuration consisting of a series of packed columns with provision for feed entry and product withdrawal from the ends of each column and with an appropriate sequence of column switching to simulate a countercurrent flow system. An important design decision is the length and number of columns in each section. This must be determined from a reliable model followed by systematic optimization study. Hence, in this work, the model is first used to evaluate the parameters and conditions for running such a reactor through a sensitivity analysis and, thereby, to guide reactor design. This is followed by computer-aided experimental characterization of the reactor performance to evaluate and validate the mathematical model. Subsequently, a systematic optimization study is performed using multiple objectives, followed by experimental verification of the optimization results. Figure 2 shows a schematic diagram of the experimental setup of the SMBR, which consists of four-jacketed stainless steel columns (0.25 m long × 0.0094 m i.d.) packed with Amberlyst 15 resin. Each column is connected to four rotary valves actuated by the control system. The four rotary valves correspond to the positions of the feed, raffinate, extract, and desorbent

streams, and they allow for either the delivery of feed/desorbent into the column or the withdrawal of raffinate/extract from the column, as required. The rotary valves are switched in tandem periodically after a preset interval (switching period), moving the positions at which the various streams enter and leave. A shift in the positions of feed and withdrawal in the direction of mobile phase flow through the bed mimics the movement of the solids in the opposite direction. It should be noted that, in the experimental study in this work, only four columns were used, although the experimental setup is very flexible because columns can be added or removed as desired without any major difficulty. The columns are arranged in a bank with the last column connected to the first so that switching of the feed, desorbent, and product streams can cycle continuously. The feed and desorbent streams are fed by HPLC pumps (Jasico, PU-1580) into the SMBR unit. The extract stream is controlled by a mass flow controller (Fisher Rosmount, QUANTIM). The raffinate stream is kept free for all the experiments to achieve periodic steady state within a reasonable experimental time.

All experiments were carried out at 318 K. During the experiments, samples from the raffinate and extract ports were collected during a particular switching time interval, and their average concentrations were analyzed by an HP 6890 gas chromatograph equipped with a 7683 automatic injector and an FID. The water concentration was measured using a volumetric Karl Fisher titrator with a model 100 titration controller from Denver Instruments.

Results and Discussion

Experiments were carried out at different switching times, feed and desorbent flow rates, and section P (feed section) flow rates. The concentration profiles for the limiting reactant (HOAc) and products (MeOAc and H_2O) within the columns were obtained from the solution of the model equations (eqs 6−11), and the performances of the SMBR were compared on the basis of performance criteria defined in eqs 12−15.

Effect of Switching Time, t_s. The switching time plays a key role in determining the performance of an SMBR unit. The effect of the switching time on the behavior of the SMBR was investigated both theoretically and experimentally. In Figure 3, results are compared for four different values of switching time. The figure reveals that the experimental results are in good agreement with the model predictions, except that the conversion of the limiting reactant (X_{HOAc}) obtained from the experiments was always higher than that predicted by the mathematical model. This is expected because the breakthrough concentration profiles of the reaction system from the single-column studies[15] also overpredicted the outlet concentration of acetic acid. Figure 3 also reveals that purity of MeOAc (P_{MeOAc}) at the raffinate port deviates from the model-predicted value when the switching time is small. This is most likely due to the nonlinear adsorption behavior of the strongly adsorbed component, water. As a result, the adsorbent requires more time to be completely regenerated, and the water remaining in the adsorbent will eventually appear in the product stream, leading to a lower P_{MeOAc}. The effect of tailing of the water concentration front on the performance of the SMBR becomes particularly obvious when the switching time is small. When the switching time was reduced from 20 min (point 2 in Figure 3) to 12 min (point 1 in Figure 3), the experimentally measured yield of MeOAc (Y_{MeOAc}) decreased from 98.2% to 42.3%, while P_{MeOAc} decreased from 97 to 79.7%. The reduction of the switching time increases the solid-phase pseudo-velocity, and therefore, all components travel at a much faster rate with the solid phase. This, in turn, reduces the residence time of the reactant and products in each section. The reduction in residence time deteriorates the performance of section R, which is responsible for desorbing the strongly adsorbed component (water) from the solid adsorbent.

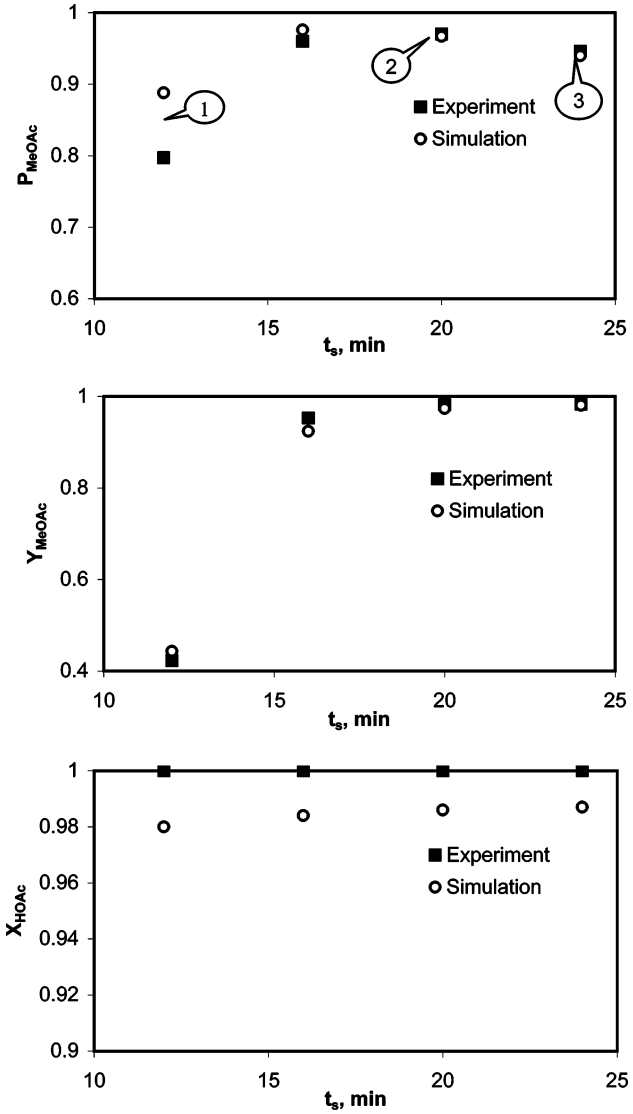

Figure 3. Effect of the switching time on the performance of the SMBR. $Q_P = 1$ mL/min, $\alpha = 0.2$, $\beta = 1.0$, $\gamma = 3.0$, $C_{HOAc} = 2$ mol/L.

The above observation can be explained from the values of σ and V, defined in eqs 16 and 17 and reported in Table 2. The table shows that countercurrent separation ($\sigma_{MeOAc} < 1$, $\sigma_{H_2O} > 1$) is achieved in sections P and S for all three points shown in Figure 3. Desorption of H_2O is better in section R (σ_{H_2O} decreases while V_{H_2O} increases) as t_s increases. This can be seen from the decreasing value of σ_{H_2O}, which changes from 0.85 to 0.51, and the increasing value of V_{H_2O}, which goes from 6.15 cmto 6.45 cm/min in section R, as shown in Table 2. As a result, more water will remain in section R at the end of the switching period for point 1 because of insufficient regeneration, and this water will eventually contaminate the product stream at the raffinate port.

Table 2. Comparison of σ and V (cm/min) Values of the Two Components MeOAc and H_2O in Different Sections for Various Operating Condition

		section P				section R				section S			
effect of	point in figure	σ_{MeOAc}	σ_{H_2O}	V_{MeOAc}	V_{H_2O}	σ_{MeOAc}	σ_{H_2O}	V_{MeOAc}	V_{H_2O}	σ_{MeOAc}	σ_{H_2O}	V_{MeOAc}	V_{H_2O}
t_s	1 in Figure 3	0.33	2.55	1.55	−1.03	0.11	0.85	6.15	0.30	0.41	3.19	1.09	−1.17
	2 in Figure 3	0.20	1.53	1.85	−0.35	0.07	0.51	6.45	0.98	0.24	1.91	1.39	−0.49
	3 in Figure 3	0.16	1.28	1.93	−0.18	0.05	0.43	6.53	1.15	0.20	1.59	1.47	−0.32
γ	1 in Figure 5	0.20	1.53	1.85	−0.35	0.13	1.02	3.00	−0.02	0.24	1.91	1.39	−0.49
	2 in Figure 5	0.20	1.53	1.85	−0.35	0.10	0.77	4.15	0.31	0.24	1.91	1.39	−0.49
	3 in Figure 5	0.20	1.53	1.85	−0.35	0.05	0.38	8.76	1.64	0.24	1.91	1.39	−0.49
α	1 in Figure 7	0.20	1.53	1.85	−0.35	0.07	0.51	6.45	0.98	0.22	1.70	1.62	−0.42
	2 in Figure 7	0.20	1.53	1.85	−0.35	0.07	0.51	6.45	0.98	0.33	2.55	0.93	−0.62
Q_P	1 in Figure 9	0.39	3.06	0.70	−0.69	0.13	1.02	3.00	−0.02	0.49	3.83	0.47	−0.75
	2 in Figure 9	0.10	0.77	4.15	0.31	0.03	0.26	13.36	2.98	0.12	0.96	3.23	0.05
	desired	<1	>1	>0	<0	<1	<1	>0	>0	<1	>1	>0	<0
		retention of H_2O				desorption of H_2O				desorption of MeOAc			

The purity and yield are poor when t_s = 12 min is primarily because of the poor regeneration of section R. When t_s is increased to 20 min, sufficient time for the regeneration of section R improves both the purity and the yield. Moreover, the increased solid-phase pseudo-velocity deteriorates the performance of section S as well, which is responsible for desorbing the weakly adsorbed component (MeOAc) and recycling it back to feed section P. This can be explained by the higher value of σ_{MeOAc} (= 0.41) for point 1 compared to the value for point 2 (= 0.24). Consequently, more MeOAc tends to be retained in section S at the end of a switching period for point 1, and This MeOAc will appear at the extract port instead of the raffinate port during the next switching period because section S becomes section R after the switch, resulting in a lower value of Y_{MeOAc}. In contrast, when the switching time was increased to 24 min (point 3 in Figure 3), the experimentally obtained P_{MeOAc} decreased slightly to 94.6%, while Y_{MeOAc} increased slightly to 99.7%. The separation factor in section P and S is important, as regeneration of the column in section R is no longer a factor. The slight decrease in ΔV (degree of separation) in sections P and S reduces both the purity and the yield. The solid-phase pseudo-velocity is reduced when the switching time is increased, and therefore, all components moved faster with the fluid phase than with the solid phase. The net separation of the concentration fronts of the two products, MeOAc and H_2O, in section P decreased (ΔV decreased from 2.2 to 2.11 cm/min), thereby deteriorating the effective separation of the two components. Consequently, water will breakthrough from section P and contaminate the product stream. However, the smaller solid-phase pseudo-velocity is beneficial for desorbing water and MeOAc in section R and section S, respectively, resulting in higher yield of MeOAc. This is expected from the increased values of V_{H_2O} from 0.98 to 1.15 in section R and V_{MeOAc} from 1.39 to 1.47 in section S. This can also be observed when the concentration profiles at the cyclic steady state are compared for the three different switching times, as shown in Figure 4. To summarize, that the purity and yield are poor when t_s is 12 min is primarily due to poor regeneration of section R. When t_s is increased to 20 min, the now-sufficient time for the regeneration of section R improves the purity and yield. However, when t_s is increased further to 24 min, the separation factor in sections P and S is important, as the regeneration of column in section R is no longer a factor. A slight decrease in ΔV (degree of separation) in sections P and S reduces both the purity and the yield.

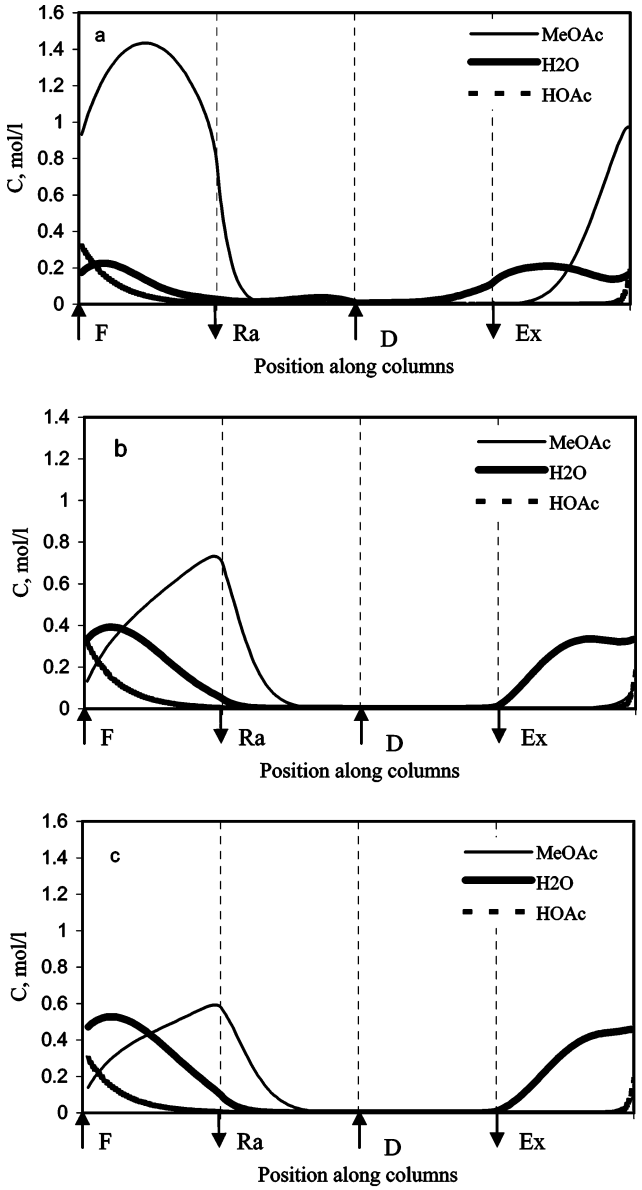

Figure 4. Effect of the switching time (t_s) on the cyclic steady-state concentration profiles of the MeOAc−H_2O−HOAc system. Q_P = 1 mL/min, α = 0.2, β = 1.0, γ = 3.0, (a) t_s = 12 min, (b) t_s = 20 min, (c) t_s = 24 min.

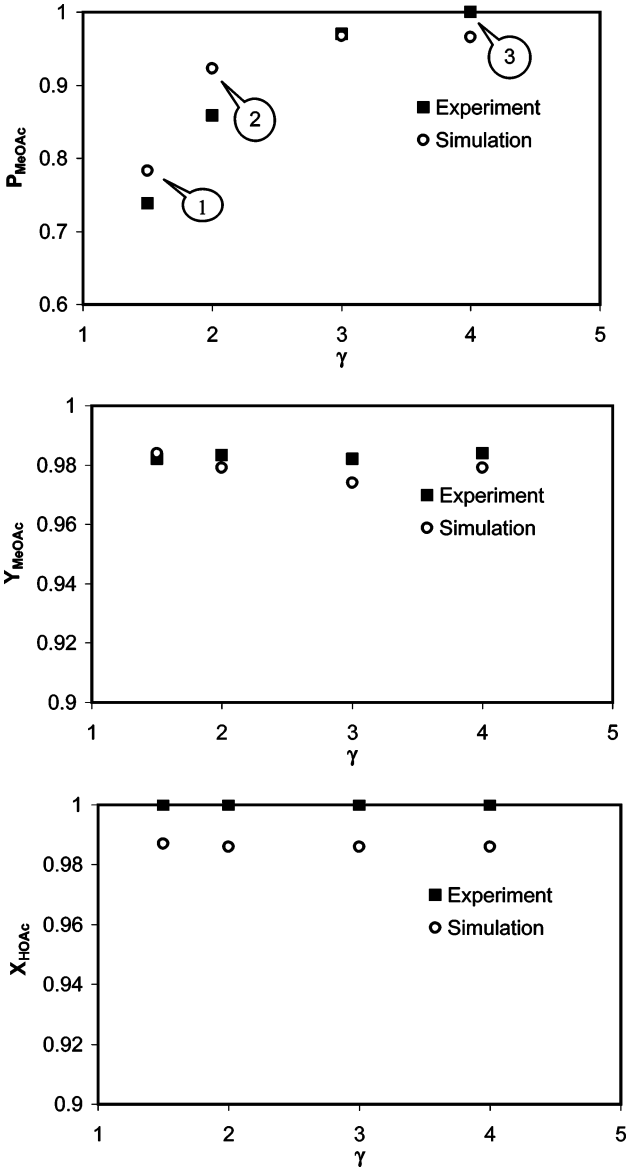

Figure 5. Effect of the desorbent flow rate (γ) on the performance of the SMBR. $Q_P = 1$ mL/min, $\alpha = 0.2$, $\beta = 1.0$, $t_s = 20$ min, $C_{HOAc} = 2$ mol/L.

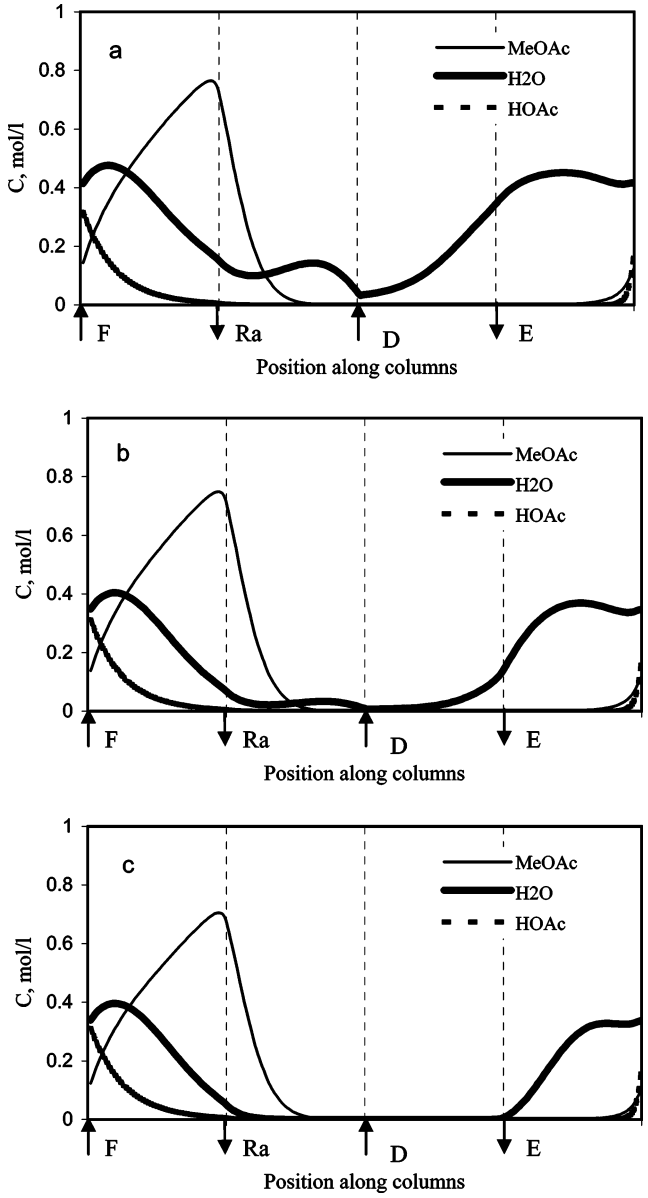

Figure 6. Effect of the desorbent flow rate (γ) on the cyclic steady-state concentration profiles of the MeOAc−H_2O−HOAc system. $Q_P = 1$ mL/min, $\alpha = 0.2$, $\beta = 1.0$, $t_s = 20$ min. (α) $\gamma = 1.5$, (b) $\gamma = 2.0$, (c) $\gamma = 4.0$.

Effect of Desorbent Flow Rate, γ. The complete regeneration of the solid adsorbent is crucial for the successful separation of the products. With a smaller switching time, water will not be completely desorbed from section R because of the tailing of its concentration front, and MeOAc will appear at the extract port because there is not enough time for MeOAc to be desorbed from section S to be recycled back to section P. On the contrary, with a longer switching time, water will break through from section P and contaminate the product stream. Therefore, the only way to further improve the separation performance is to completely regenerate (purge) at least one column in section R by increasing the desorbent (solvent) flow rate.

Figure 5 shows the effect of the desorbent flow rate (γ) on the performance of the SMBR. It is obvious that the model can predict the experimental results quite well at different desorbent flow rates. The model over-predicts the experimental results for P_{MeOAc} at lower desorbent flow rates, whereas it underpredicts P_{MeOAc} at higher flow rates. This is possibly due to the nonlinear adsorption behavior of the strongly adsorbed component, water. To achieve the same regeneration performance, a higher desorbent flow is required than that predicted from the linear model. The prediction for Y_{MeOAc} is very good in the range of solvent flow rates studied. However, the model-predicted value of X_{HOAc} is always lower than the experimental values, which shows that complete conversion of HOAc is possible in an SMBR. It is observed that P_{MeOAc} at the raffinate port is improved by a higher rate of eluent flow, although Y_{MeOAc} is hardly changed. This can be explained by comparing the steady-state concentration profiles for γ equal to 1.5, 2.0, and 4.0 shown in Figure 6. When γ is 1.5, a considerable amount of water breaks through at the raffinate port because of inadequate desorption of water (purging) in section R [$\sigma_{H_2O} > 1$ (Table 2), so water still moves with the solid phase]. This is indeed found to be true as, when γ is increased to 2, P_{MeOAc} increases significantly because of the better regeneration of the solid phase in section R ($\sigma_{H_2O} = 0.77$) at the end of a switching period. When γ is further increased to 4.0,

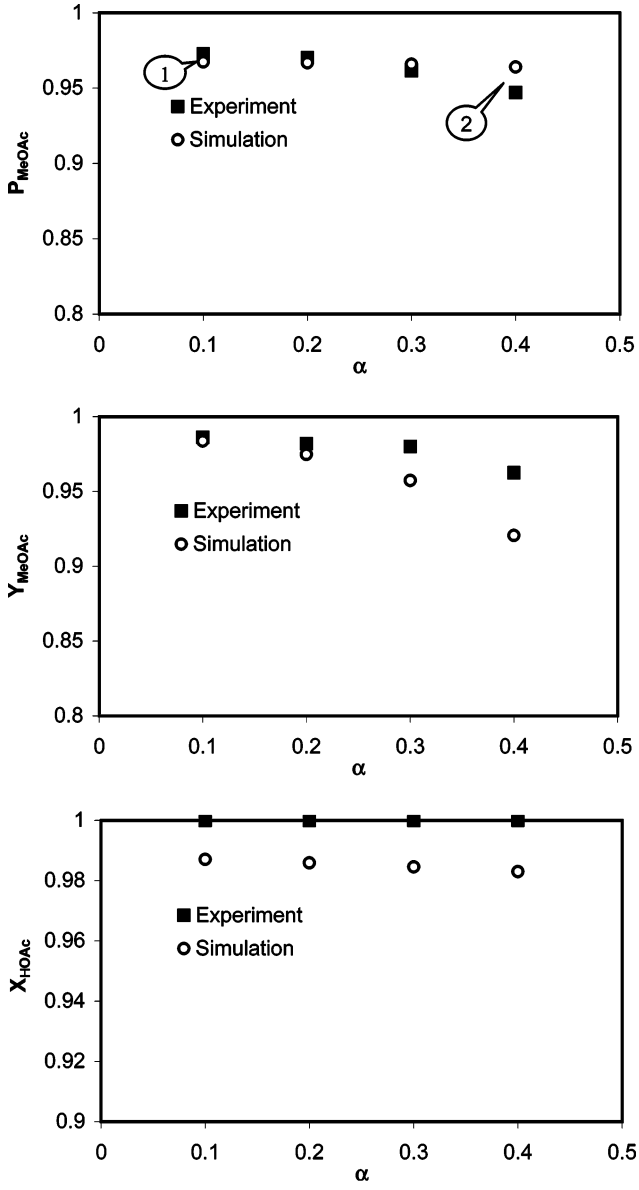

Figure 7. Effect of feed flow rate (α) on the performance of the SMBR. $Q_P = 1$ mL/min, $\beta = 1.0$, $\gamma = 3.0$, $t_s = 20$ min, $C_{HOAc} = 2$ mol/L.

hardly any water appears at the raffinate port because, at this high eluent flow rate, section R is almost completely free of water ($\sigma_{H_2O} = 0.38$). Therefore, increasing γ and keeping all of the other parameters fixed improves the regeneration of section R (decreasing σ_{H_2O} and increasing V_{H_2O}), resulting in better purity. It should noted that the improvement of P_{MeOAc} becomes less significant when the desorbent flow rate becomes sufficiently large.

Effect of Feed Flow Rate, α. The effect of the feed flow rate on the performance of the SMBR is illustrated in Figure 7. It was found that the purity and yield of MeOAc decreased with increasing feed flow rate, α. Because the flow rate in section P (Q_P) is fixed and because Q_S is equal to $(1 - \alpha)Q_P$, the increase of the feed flow rate leads to a reduction in the fluid flow rate in section S. The smaller fluid-phase velocity in section S deteriorates its performance in desorbing MeOAc, as can be seen in Table 2, where the value of V_{MeOAc} decreased from 1.62 to 0.93, which is equivalent to increasing the solid-phase pseudo-velocity by reducing

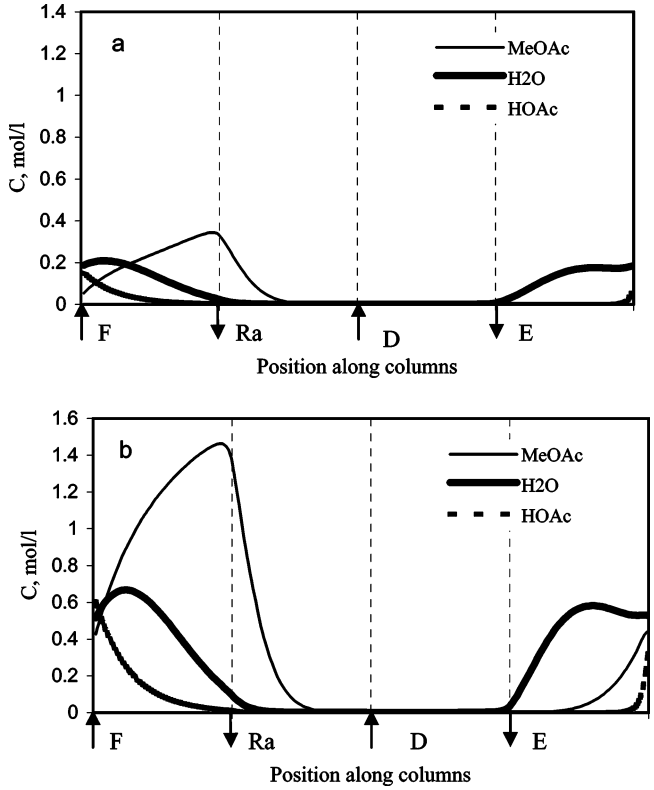

Figure 8. Effect of the feed flow rate (α) on the on the cyclic steady-state concentration profiles of the MeOAc−H_2O−HOAc system. $Q_P = 1$ mL/min, $\beta = 1.0$, $\gamma = 3.0$, $t_s = 20$ min. (α) $\alpha = 0.1$, (b) $\alpha = 0.4$.

the switching time. More MeOAc and unreacted HOAc will be retained in section S at the end of a switching period, and the remaining components will break through at the extract port during the next switching period when section S becomes section R. As the feed flow rate was increased, P_{MeOAc} in the raffinate decreased slightly. Because more water is likely to be produced at a higher feed flow rate, the performance of the adsorbent regeneration deteriorates unless the desorbent flow rate is increased. This will be greater because of the nonlinear behavior of the strongly adsorbed component, water. The remaining water in the adsorbent will eventually appear at the raffinate port, leading to a lower product purity. Moreover, as α was increased from 0.1 to 0.4 while all other parameter values were kept constant, ΔV (effective separation factor) in section S decreased significantly from 2.04 to 1.55 (see Table 2), lowering both the purity and the yield. This can be illustrated by comparing the steady-state concentration profiles for two different feed flow rates, as shown in Figure 8.

Effect of Flow Rate in Section P, Q_P. The effect of the flow rate in section P on the behavior of the SMBR is demonstrated in Figure 9. The fluid-phase velocity in each section is increased with increasing flow rate in section P (Q_P). The higher fluid-phase velocity is beneficial for the performance of sections R and S, which are responsible for desorbing water and MeOAc, respectively. However the increased fluid-phase flow rate deteriorates the performance of section P, which plays the central role in the reaction and separation of the products for MeOAc synthesis in the SMBR. On one hand, when the fluid-phase flow rate is increased, the residence time is not sufficient for acetic acid to be completely consumed. Hence, the unconverted acid will break through from the raffinate port because it has an

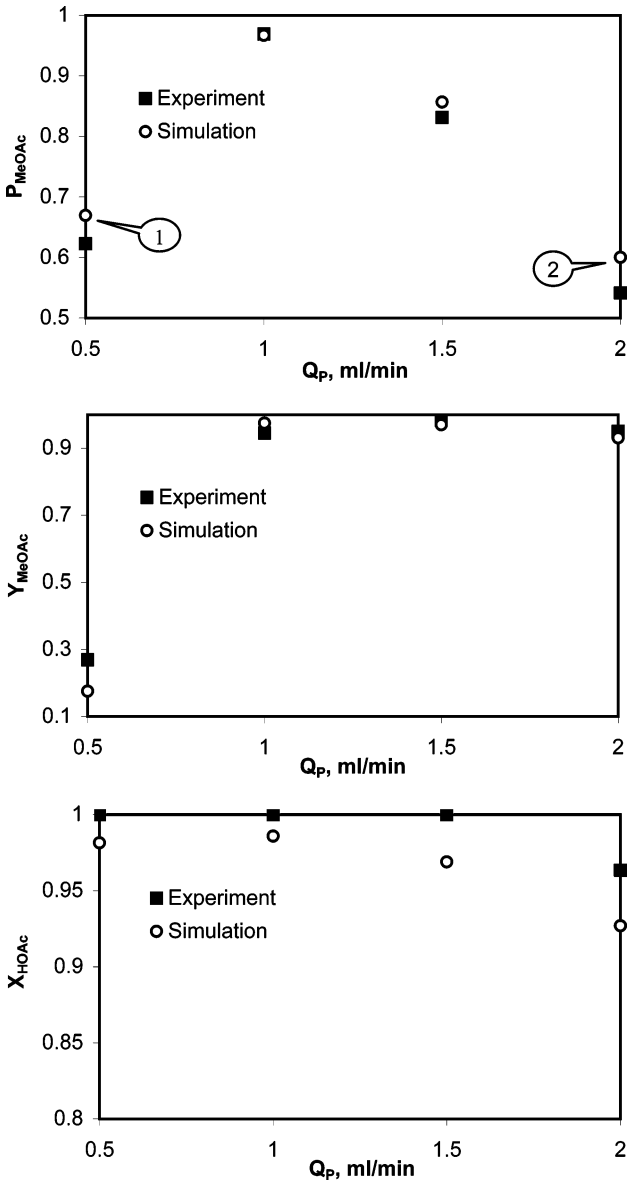

Figure 9. Effect of the flow rate in section P (Q_P) on the performance of the SMBR. $\alpha = 0.2$, $\beta = 1.0$, $\gamma = 3.0$, $t_s = 20$ min, $C_{HOAc} = 2$ mol/L.

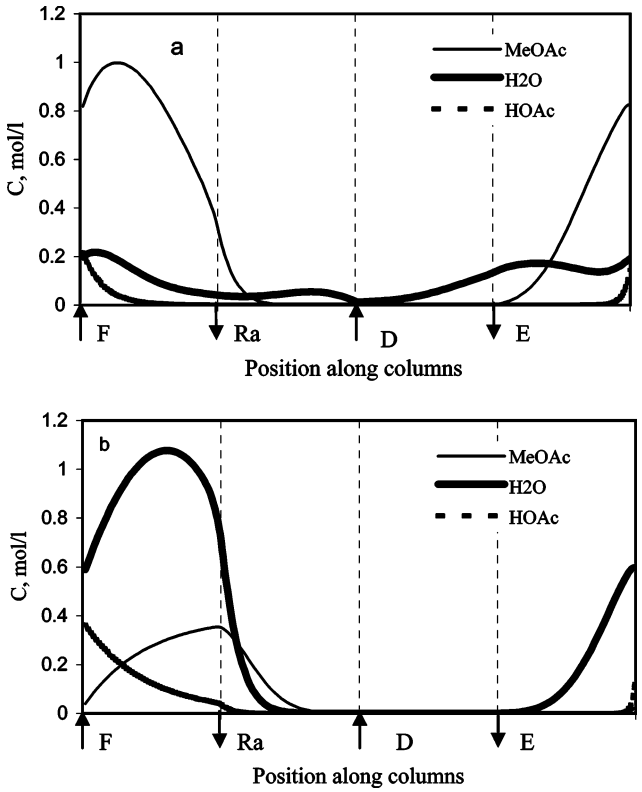

Figure 10. Effect of the flow rate in section P (Q_P) on the cyclic steady-state concentration profiles of the MeOAc−H_2O−HOAc system. $\alpha = 0.2$, $\beta = 1.0$, $\gamma = 3.0$, $t_s = 20$ min. (a) $Q_P = 0.5$ mL/min, (b) $Q_P = 2.0$ mL/min.

adsorption affinity toward the resin that is similar to that of MeOAc, and therefore, the product stream would be contaminated. On the other hand, if Q_P is small, water tends to break through from at the raffinate port.

When the flow rate in section P was decreased from 1 mL/min to 0.5 mL/min, the P_{MeOAc} and Y_{MeOAc} were decreased significantly from 97 and 98.2% to 62.3 and 26.9%, respectively. This is probably because of the decrease of ΔV (degree of separation) from 2.2 to 1.39 (see Table 2) in section P and from 1.88 to 1.22 in section S. Moreover, the desorption of water in section R ($\sigma_{H_2O} > 1$, water still moves with the solid phase) and the desorption of methyl acetate in section S (V_{MeOAc} decreased from 1.39 to 0.47) are poor because of the decreased fluid-phase velocity. This can also be seen when the concentration profiles are compared, as in Figures 10a and 4b. At low Q_P, a large amount of water is retained in section R ($\sigma_{H_2O} = 1.02$), which eventually pollutes the product stream at the raffinate port (see Figure 10a). MeOAc and unconverted HOAc are kept in section S at the end of a switching period and will ultimately be lost with the extract stream during the next switching period lowering the Y_{MeOAc}.

When the flow rate in section P was increased to 2 mL/min, P_{MeOAc} once again decreased dramatically from 97 to 54%, whereas the Y_{MeOAc} decreased slightly. As shown in Figures 10b and 4b, when the fluid flow rate is increased in section P, water tends to break through from the raffinate port, lowering the purity significantly [$\sigma_{H_2O} < 1$ in both section P ($\sigma_{H_2O} = 0.77$) and section S ($\sigma_{H_2O} = 0.96$) when Q_P is 2 mL/min, and therefore, water moves with the fluid phase cocurrently and not countercurrently] unless the switching time is changed. The reduced residence time also lowers the conversion of acetic acid, and the unconverted acetic acid will elute with the fluid phase at the raffinate port, leading to a lower product purity, P_{MeOAc}. Although ΔV in section S increases from 1.88 to 3.28 when Q_P is increased to 2.0 mL/min, the yield decreases slightly because $\sigma_{H_2O} < 1$ and $V_{H_2O} > 1$ in section S.

Sensitivity Study. The experimental results, as well as the theoretical model, clearly demonstrate that it is possible to obtain improved conversions and product purities for methyl acetate synthesis in an SMBR. In addition, it was found that the model adequately predicts the experimentally observed overall performance of the reactor for changing values of various operating variables. This also verifies that the adsorption and kinetic parameters previously obtained experimentally[15] are correct and that the model is quite robust and reliable. An important design decision for an SMBR is the appropriate length (L_{col}) and number (N_{col}) of columns in each section, as well as various flow rates. These parameters must be determined from a systematic optimization study. The effects of the switching time, the desorbent and feed flow rates, and the flow

Table 3. Sensitivities of Process Parameters for the Synthesis of MeOAc[a]

	Y_{MeOAc}	P_{MeOAc}	X_{HOAc}	S_{MeOAc}
t_s	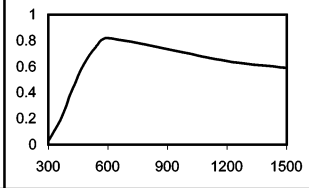	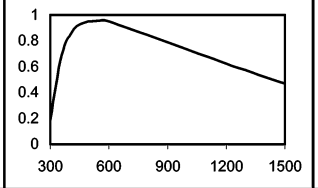	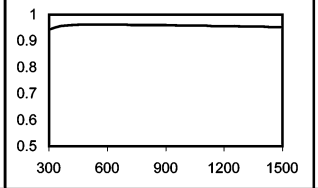	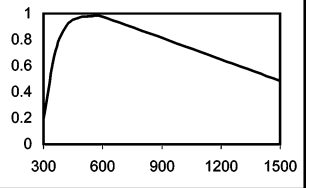
Q_P	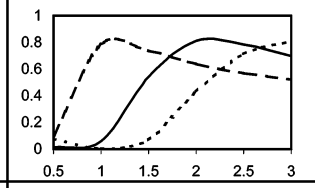	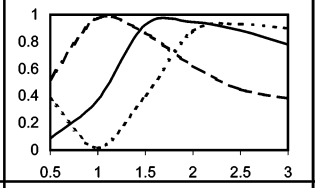	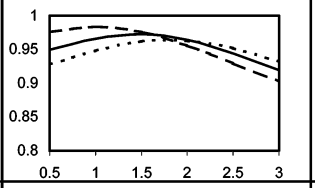	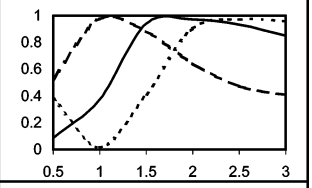
α	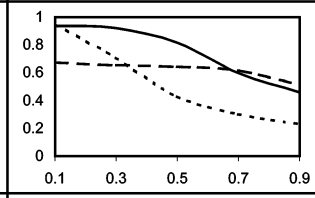	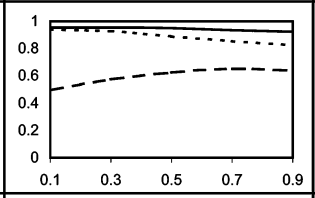	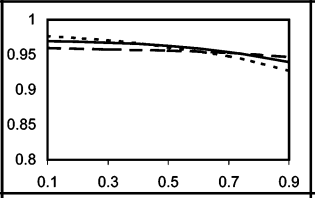	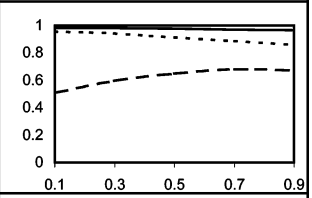
β	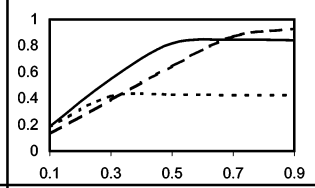	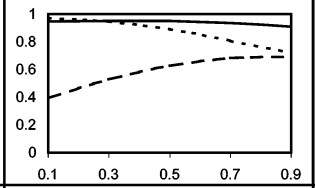	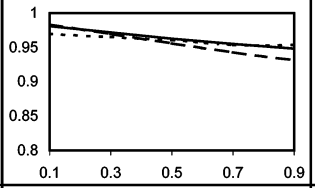	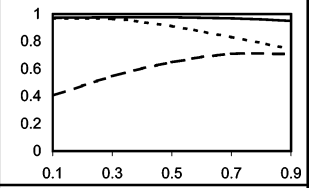
γ	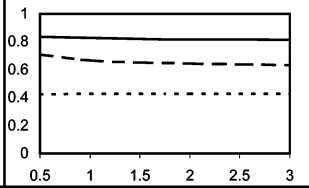	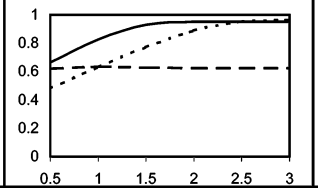	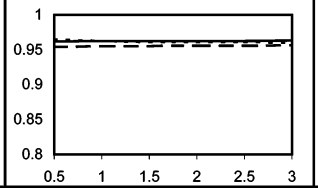	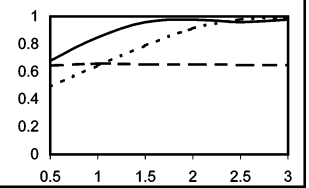
p	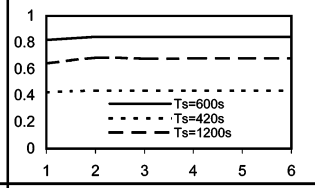	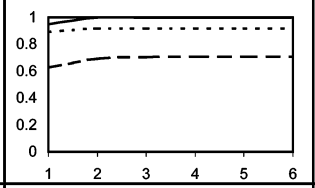	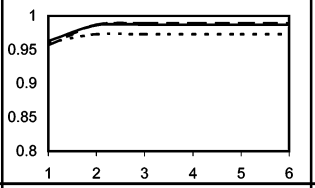	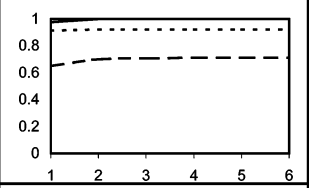
q	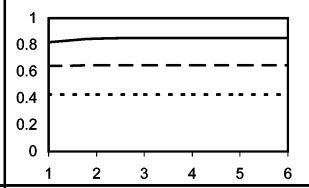	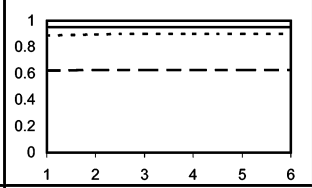	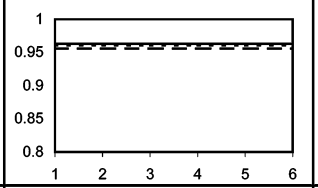	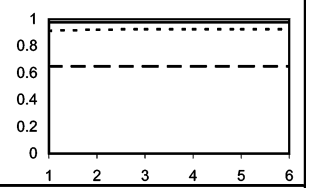
r	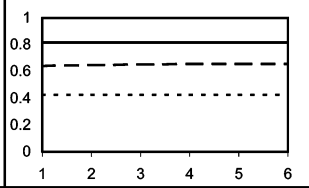	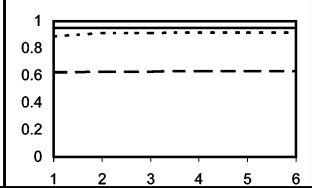	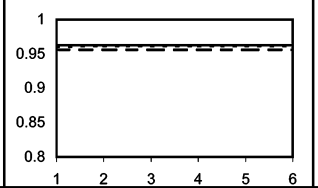	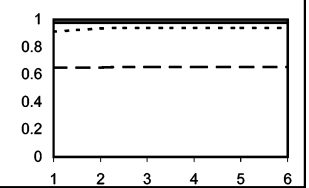
s	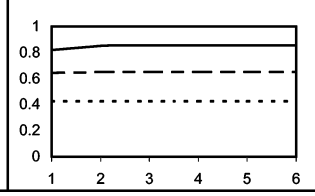	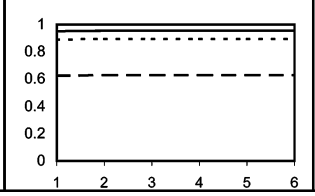	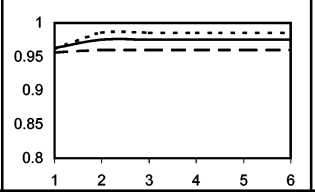	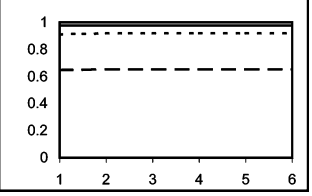

[a] Reference values: $p = 1$, $q = 1$, $r = 1$, $s = 1$, $Q_P = 2$ mL/min, $L = 25$ cm, $\epsilon = 0.4$, $[HOAc]_f = 2$ mol/L, $\alpha = 0.5$, $\beta = 0.5$, $\gamma = 2.0$.

rate in section P on the performance of the SMBR revealed that there is a complex interplay among all of these operating parameters in terms of their impacts on X_{HOAc}, Y_{MeOAc}, S_{MeOAc}, and P_{MeOAc}. A close scrutiny of all of the figures presented here clearly reveals that, if we want to maximize one output parameter (for example, Y_{MeOAc}), another one (for example, P_{MeOAc}) worsens (e.g., see Figure 5). Therefore, a comprehensive parametric sensitivity study must be conducted to acquire a thorough understanding of the SMBR system.

A sensitivity analysis was carried out by changing only one process parameter at a time while fixing the other operating parameters at a reference set of values. Table 3 shows the results of the sensitivity study. The effects of the switching time (t_s); flow rates of feed (α), raffinate (β), and desorbent (γ); flow rate in section P (Q_P); and numbers of columns (p, q, r, and s) in sections P, Q, R, and S, respectively, on the several performance criteria, namely, Y_{MeOAc}, P_{MeOAc}, X_{HOAc}, and S_{MeOAc}, as defined in eqs 12−15, are shown. The parameters in the left column of Table 3 denote the x-axis variable for the respective row, and the effects of each parameter on Y_{MeOAc}, P_{MeOAc}, X_{HOAc}, and S_{MeOAc} are shown for reference values of the other parameters in the four subsequent columns. The effect of switching time, t_s, is shown in the diagrams in the first row. Subsequently, three values of t_s (420, 600, and 1200 s) were used to show the influence of a particular parameter on Y_{MeOAc}, P_{MeOAc}, X_{HOAc}, and S_{MeOAc}.

It was found that q and r, which represent the numbers of columns in sections Q and R, respectively, have little effect on the performance of the process, for values between 1 and 6. Some parameters, such as β and γ, influence Y_{MeOAc}, P_{MeOAc}, X_{HOAc}, and S_{MeOAc} in conflicting ways. Moreover, the effects of α, β, γ, and p are quite different depending on the switching time. The influence of the switching time is particularly complex, as its optimum value depends not only on the distribution of columns, but also on the values of α, β, and γ. A close look at Table 3 reveals that there is an intricate relationship among the effects of all of these parameters on Y_{MeOAc}, P_{MeOAc}, X_{HOAc}, and S_{MeOAc}. If we want to optimize one, another one worsens. The optimum SMBR configuration (number and length of columns) and operating conditions (such as t_s, β, γ, etc.) differ depending on which performance variable we want to maximize among Y_{MeOAc}, P_{MeOAc}, X_{HOAc}, and S_{MeOAc}, and it might not be possible to maximize all at the same time. One might also obtain infinitely many optimal solutions, or Pareto optimal solutions, when one performs a multiobjective optimization of an SCMCR. Pareto optimal solution is usually obtained when one or more of the decision variables are conflicting in nature. This is indeed found for this system, as discussed elsewhere.[21]

Conclusions

The synthesis of methyl acetate (MeOAc) in a simulated moving bed reactor (SMBR) was investigated by numerical simulation as well as experiment. A rigorous mathematical model was developed to describe the dynamic behavior of the SMBR, and comparison with the experimental results obtained at various operating conditions further validated the model. It was observed that the predicted results were in good agreement with those found from experiment. A high yield and purity of MeOAc and near-complete conversion of the limiting reactant, acetic acid, could be achieved in SMBR by selecting proper operating conditions. A parametric analysis was carried out on the verified model to systematically investigate the effects of the process parameters on the performance of the SMBR. It was found that there is a complex interaction of all these parameters on the reactor performance. Some of the operating parameters not only influence the purity, yield, and selectivity of MeOAc significantly, but also act in conflicting ways. This makes selection of the length and number of columns in various sections, the switching time, and the flow rates in different sections extremely difficult because a desirable change in one performance criterion results in an unfavorable change in another desired variable. Therefore, one must carry out a systematic multiobjective optimization study using the experimentally verified model developed in this study to determine the appropriate design and successful implementation of an SMBR on an industrial scale.

Notation

C = liquid-phase concentration, mol/l
D = desorbent, apparent axial dispersion coefficient, m^2/s
k = reaction rate constant
K = equilibrium constant
L = column length, m
N = number of switchings
p = number of columns in section P
P = purity, section P
q = solid-phase concentration, number of columns in section Q
Q = volume flow rate, section Q, cm^3/min
r = number of columns in section R
R = reaction rate, section R
s = number of columns in section S
S = selectivity, section S
t = time, min
T = temperature, K
u = superficial velocity, m/s
V = velocity, m/s
X = conversion
Y = yield
z = axial coordinate, cm

Greek Letters

α = fraction of feed
β = fraction of raffinate
γ = fraction of desorbent
δ = phase ratio
ϵ = void fraction
ϕ = section
σ = relative carrying capacity
ζ = solid-phase pseudo-velocity

Subscripts/Superscripts

o = initial, inlet
col = column
e = equilibrium
E = extract
f = feed, forward
i = component i
j = column number
g = gas, carrier
HOAc = acetic acid
MeOAc = methyl acetate
N = number, switching period
P = section P
Q = section Q
R = section R
S = switching, section S, solid

Literature Cited

(1) Mazzotti, M.; Kruglov, A.; Neri, B.; Gelosa, D.; Morbidelli, M. A. Continuous chromatographic reactor: SMBR. *Chem. Eng. Sci.* **1996**, *51*, 1827.

(2) Kawase, M.; Suzuki, T. B.; Inoue, K.; Yoshimoto, K.; Hashimoto, K. Increased esterification conversion by application of the simulated moving-bed reactor. *Chem. Eng. Sci.*, **1996**, *51*, 2971.

(3) Migliorini, C.; Fillinger, M.; Mazzotti, M.; Morbidelli, M. Analysis of simulated moving bed reactors. *Chem. Eng. Sci.* **1999**, *54*, 2475.

(4) Dunnebier, G.; Fricke, J.; Klatt, K. Optimal design and operation of simulated moving bed chromatographic reactors. *Ind. Eng. Chem. Res.* **2000**, *39*, 2290.

(5) Lode, F.; Houmard, M.; Migliorini, C.; Mazzotti, M.; Morbidelli, M. Continuous reactive chromatography. *Chem. Eng. Sci.* **2001**, *56*, 269.

(6) Zhang, Z.; Hidajat, K.; Ray, A. K. Application of Simulated Countercurrent Moving Bed Chromatographic Reactor for MTBE Synthesis. *Ind. Eng. Chem. Res.* **2001**, *40*, 5305.

(7) Ray, A. K.; Tonkovich, A.; Carr, R. W.; Aris, R. The simulated countercurrent moving bed chromatographic reactor: A novel reactor−separator. *Chem. Eng. Sci.* **1990**, *45*, 2431.

(8) Ray, A. K.; Carr, R. W.; Aris, R. The simulated countercurrent moving-bed chromatographic reactor—a novel reactor−separator. *Chem. Eng. Sci.* **1994**, *49*, 469.

(9) Ray, A. K.; Carr, R. W. Experimental study of a laboratory scale simulated countercurrent moving bed chromatographic reactor. *Chem. Eng. Sci.* **1995**, *50*, 2195.

(10) Ray, A. K.; Carr, R. W. Numerical simulation of a simulated countercurrent moving bed chromatographic reactor. *Chem. Eng. Sci.* **1995**, *50*, 3033.

(11) Hashimoto, K.; Adachi, S.; Noujima, H.; Ueda, Y. A New Process Combining Adsorption and Enzyme Reaction for Producing Higher Fructose Syrup. *Biotechnol. Bioeng.* **1983**, *25*, 2371.

(12) Ching, C. B.; Lu, Z. P. Simulated Moving-Bed Reactor: Application in Bioreaction and Separation. *Ind. Eng. Chem. Res.* **1997**, *36*, 152.

(13) Meurer, M.; Altenhoner U.; Strube, J.; Untiedt A.; Schmidt-Traub, H. Dynamic simulation of a Simulated-Moving-Bed Chromatographic Reactor for the Inversion of Sucrose. *Starch/Starke* **1996**, *48*, 452.

(14) Azevedo, D. C. S.; Rodrigues, A. E. Design methodology and operation of a simulated moving bed reactor for the inversion of sucrose and glucose-fructose separation. *Chem. Eng. J.* **2001**, *82*, 95.

(15) Yu, W.; Hidajat, K.; Ray, A. K. Determination of kinetic and adsorption parameters for methyl acetate esterification and hydrolysis reaction catalyzed by Amberlyst 15, in press, *Appl. Catal. A: Gen.* 2003.

(16) Mazzotti, M.; Neri, B.; Gelosa, D.; Kruglov, A.; Morbidelli, M. Kinetics of Liquid-Phase Esterification Catalyzed by Acidic Resins. *Ind. Eng. Chem. Res. 36*, **1997**, *26*, 3.

(17) Zhang, Z.; Hidajat, K.; Ray, A. K. Determination of adsorption and kinetic parameters for methyl *tert*-butyl ether synthesis from *tert*-butyl alcohol and methanol. *J. Catal.* **2001**, *200*, 209.

(18) Petroulas, T.; Aris, R.; Carr, R. W. Analysis and performance of a countercurrent moving-bed chromatographic reactor. *Chem. Eng. Sci.* **1985**, *40*, 2233.

(19) Fish, B.; Carr, R. W.; Aris, R. The continuous countercurrent moving bed chromatographic reactor. *Chem. Eng. Sci.* **1986**, *41*, 661.

(20) Ruthven, D. M. The axial dispersed plug flow model for continuous counter-current adsorbers. *Can. J. Chem. Eng.* **1983**, *61*, 881.

(21) Yu, W.; Hidajat, K.; Ray, A. K. Multiobjective optimization of reactive SMB and Varicol process for methyl acetate synthesis. *Ind. Eng. Chem. Res.* **2003**, in press.

Received for review March 10, 2003
Revised manuscript received September 22, 2003
Accepted September 29, 2003

IE0302241